Thermodynamic Model for Nonlinear Electrostatic Adsorption Equilibrium of Protein

Xue-Li Su and Yan Sun
Dept. of Biochemical Engineering, School of Chemical Engineering and Technology, Tianjin University, Tianjin 300072, China

DOI 10.1002/aic.10900
Published online June 16, 2006 in Wiley InterScience (www.interscience.wiley.com).

A statistical thermodynamic model is developed for the nonlinear multicomponent protein adsorption equilibrium on ion exchanger. This model takes into account the electrostatic interactions between the adsorbent surface and protein molecules, as well as the lateral interactions between adsorbed protein molecules. The model is, therefore, in accord with the nonstoichiometric nature of the electrostatic adsorption of protein. There are two categories of model parameters: one corresponds to the adsorption affinity of the protein and the other is descriptive of the interactions between the adsorbed molecules. So, all the model parameters have definite physical meanings, and for the adsorption equilibria of single protein, there are only two model parameters. By comparison with batch adsorption equilibrium data of bovine serum albumin, the model is found to fit the experimental data well. The effects of buffer type, pH and ionic strength on the model parameters are reasonably interpreted by the electrostatic and thermodynamic theories.
 AIChE J, 52: 2921–2930, 2006
Keywords: electrostatic adsorption; chromatography; statistical thermodynamics; non-stoichiometric model; ion exchange.

Introduction

Liquid chromatography, based on the interactions between charged solutes and ionized ligands is usually known as ion-exchange chromatography. Ion-exchange chromatography is widely used in the analysis and purification of proteins, because the adsorption can be readily modulated by mobile phase ionic strength. Adsorption equilibrium is of fundamental interest in the design and optimization of chromatographic processes, as well as in the evaluation of adsorbents. Up to now, there have been a few equilibrium models proposed for ion-exchange adsorption of proteins, such as Langmuir model,[1] stoichiometric displacement model,[2] nonideal surface solution (NISS) model,[3] steric mass-action (SMA) model,[4] and SMA-NISS model.[5] These models are all based on a stoichiometric ion-exchange mechanism, and most of the model formulas are in simple form. Hence, the models can be readily used for general analysis of adsorption and chromatography processes, and new development continues to be attained based on the theories. However, it should be emphasized that the theoretical basis of the models is not completely realistic because the so-called "ion exchange" is really based on electrostatic interactions, and the long-range electrostatic interactions do not follow the stoichiometric law.[6] For example, Haggerty and Lenhoff found an excellent correlation between the mean surface potential and the retention time of proteins,[7] indicating the nonstoichiometric nature of the so-called ion-exchange adsorption of protein. Hence, development of a mechanistic model is a current challenge on the protein adsorption theory on ion exchangers.

A variety of approaches have been adopted in the quest for realistic mechanistic adsorption equilibrium models. For example, the models proposed by Norde and Lyklema[8,9] took into account protein-adsorbent electrostatic contribution by treating the adsorbed protein as a flat sheet comprising multiple planar layers, differing in dielectric constant and charge distribution.

Correspondence concerning this article should be addressed to Y. Sun at ysun@tju.edu.cn.

In the work of Roth and Lenhoff,[10] which considered protein-adsorbent interactions (electrostatic interaction and van der Waals interaction), the Gibbs approach to adsorption that involves surface excess and distribution of concentrations from the adsorption interface out to the bulk solution was employed. These models were in accord with the nonstoichiometric nature of electrostatic interaction. However, they ignored the interplay between adsorbed protein molecules, and were only applicable to linear adsorption at low-protein concentrations. More recently, a new isotherm from another perspective, the available area isotherm,[11] was presented for nonlinear adsorption equilibrium of proteins. The model had a better thermodynamic foundation, but the interactions of the adsorbed proteins were not considered. Hence, the above models possess a serious limitation in protein adsorption modeling, in view of the high adsorption amount often encountered in preparative chromatography when lateral interactions between adsorbed proteins are important.

In this work, a statistical thermodynamic (ST) model is developed for the nonlinear multi-component protein adsorption equilibrium on ion-exchanger. The model is based on the statistical thermodynamic theory and takes into consideration of the lateral interactions between adsorbed protein molecules. The model takes a form of nonlinear equation with two categories of model parameters with definite physical meanings. The validity of the model is demonstrated using batch adsorption equilibrium data of bovine serum albumin (BSA) to DEAE Spherodex M under different conditions.

Theory

This chapter is devoted to the theoretical development of the nonlinear multicomponent protein adsorption equilibrium between the adsorption phase (ion exchanger) and bulk protein solution. The adsorption equilibrium theory is derived on the basis of thermodynamics, and the following fundamental hypotheses:

1. The adsorption phase is composed of counterions, coions, solvent molecules and adsorbed protein molecules.
2. All molecules distribute uniformly in the adsorption phase.
3. The interaction potential between protein molecules and the adsorption interface is independent of the position in adsorption phase and protein adsorption amount.
4. All molecules in the adsorption phase undergo equal short-range interactions.
5. Bulk protein solution is considered ideal because of its low-concentration nature.
6. Protein molecules are regarded as spheres.
7. The adsorption phase has the same volume as that of the pores in the matrix material of the ion exchanger, because the adsorption occurs in the volume of the pores for the ion exchanger of DEAE Spherodex M used in this work (see the following for the Experimental chapter).

In the adsorption phase, all components are distinguished by subscripts of 1 to $n+3$ that refer to n species of proteins, counter-ions, co-ions and solvent molecules, respectively. The chemical potential of protein i in the adsorption phase (μ_i^s) comprises two parts: the contribution of interactions between molecules in the adsorption phase $\mu_i^{s'}$ and that of interactions between protein and adsorption interface ε_{is}, so

$$\mu_i^s = \mu_i^{s'} + \varepsilon_{is} \tag{1}$$

The adsorption phase is a system of constant temperature (T), volume (V) and molecule number (N_i). According to thermodynamic theory

$$\mu_i^{s'} = N_A\left(\frac{\partial A}{\partial N_i}\right)_{T,V,N_{j\neq i}} = -RT\left(\frac{\partial \ln Z}{\partial N_i}\right)_{T,V,N_{j\neq i}}, (i = 1, \ldots n) \tag{2}$$

where Z is the canonical partition function excluding the contribution of protein-adsorbent interaction. Thus, $\mu_i^{s'}$ can be determined with a proper expression for Z. In a cell theory of liquids of the statistical thermodynamics, the volume of liquid is divided into a lattice of cells, with one molecule in each cell. Each molecule is in the potential field of other molecules and can move within its cell. Based on the assumptions of similar molecular size and random molecular distribution, the liquid cell theory expresses Z as[12]

$$Z = \frac{(\Sigma_{j=1,\ldots,n+3} N_j)!}{\Pi_{j=1,\ldots,n+3} N_j!} \times \exp\left(-\frac{\bar{W}}{k_B T} + \sum_{i=1,\ldots,n+3} N_i\right) \prod_{j=1,\ldots,n+3} \left(\frac{\nu_{fj}}{\Lambda_j^3}\right)^{N_j} \tag{3}$$

where $\bar{W}$ is the mean configurational potential energy, with each molecule at the center of its cell. $\bar{W}$ comprises the contributions of both long-range electrostatic interaction ($\bar{W}_{ele}$) and short-range interaction ($\bar{W}_{sh}$). In the adsorption phase, the electrostatic interactions of protein-protein, ion-ion and ion-protein all contribute to $\bar{W}_{ele}$. Since the electrostatic interaction of protein-protein ($\bar{W}_{ele,pp}$) is commonly treated as the change in the free energy of the system as the protein molecules move from infinite separation to the actual distance in the solution,[13] the change of ion-ion and ion-protein electrostatic interaction potential, which is one part of free energy change of the system, is included in $\bar{W}_{ele,pp}$. Therefore

$$\bar{W}_{ele} = \bar{W}_{ele}^{\inf} + \bar{W}_{ele,pp} = \bar{W}_{ele}^{\inf} + \sum_{i=1,\ldots,n} \frac{1}{2}\varepsilon_{ele,i} N_i \tag{4}$$

where $\bar{W}_{ele}^{\inf}$ is the contribution of electrostatic interaction to the mean configurational potential energy when protein molecules are infinitely apart, and $(1/2)\varepsilon_{ele,i}$ is the mean electrostatic interaction potential of each molecule of protein i.

From model hypothesis (4), we express $\bar{W}_{sh}$ as

$$\bar{W}_{sh} = \frac{1}{2}\varepsilon_{sh} \sum_{i=1,\ldots,n+3} N_i \tag{5}$$

where $(1/2)\varepsilon_{sh}$ is the mean short-range interaction potential of each molecule. Combining Eqs. 4 and Eq. 5 yields the following relationship

$$\bar{W} = \bar{W}_{ele} + \bar{W}_{sh} = \bar{W}_{ele}^{\inf} + \sum_{i=1,\ldots,n} \frac{1}{2}\varepsilon_{ele,i}N_i + \frac{1}{2}\varepsilon_{sh}\sum_{i=1,\ldots,n+3} N_i \quad (6)$$

Because

$$\varepsilon_{ele,i} \approx \sum_{j=1,\ldots,n} \eta_{ij}\int_V \rho_j(r)u_{ij}(r)4\pi r^2 dr = \sum_{j=1,\ldots,n} \eta_{ij}N_j\frac{\int_V u_{ij}(r)4\pi r^2 dr}{V_j} \quad (i = 1, \ldots, n) \quad (7)$$

Eq. 6 can be rewritten as

$$\bar{W} = \bar{W}_{ele}^{\inf} + \sum_{i=1,\ldots,n}\sum_{j=1,\ldots,n}\frac{1}{2}\eta_{ij}N_iN_j\frac{\int_V u_{ij}(r)4\pi r^2 dr}{V_j} + \frac{1}{2}\varepsilon_{sh}\sum_{i=1,\ldots,n+3} N_i \quad (8)$$

where η_{ij} is the correction factor for the contribution of long-range electrostatic interaction potential between proteins i and j due to the difference in their adsorption space, which is a parameter only dependent on the characteristics of adsorbent and proteins i and j.

Omitting the changes of ν_{fj} with molecule number, we obtain the following relationship from Eqs. 2, 3 and 8, with model hypothesis (4), that indicates the independence of ε_{sh} on N_i

$$\mu_i^{s'} = RT\ln N_i - RT - RT\ln\left(\frac{\nu_{fi}}{\Lambda_i^3}\right) + \frac{1}{2}N_A\varepsilon_{sh} + N_A\sum_{j=1,\ldots,n}\eta_{ij}N_j\frac{\int_V u_{ij}(r)4\pi r^2 dr}{V_j} \quad (9)$$

Because $N_j = N_AV_jq_j$,, Eq. 9 can be rewritten as

$$\mu_i^{s'} = RT\ln(N_AV_i) + RT\ln q_i - RT - RT\ln\left(\frac{\nu_{fi}}{\Lambda_i^3}\right) + \frac{1}{2}N_A\varepsilon_{sh} + N_A^2\sum_{j=1,\ldots,n}\eta_{ij}q_j\int_V u_{ij}(r)4\nu r^2 dr \quad (10)$$

Thus, combining Eqs. 1 and 10 gives

$$\mu_i^{s} = RT\ln(N_AV_i) + RT\ln q_i - RT - RT\ln\left(\frac{\nu_{fi}}{\Lambda_i^3}\right) + \frac{1}{2}N_A\varepsilon_{sh} + N_A^2\sum_{j=1,\ldots,n}\eta_{ij}q_j\int_V u_{ij}(r)4\pi r^2 dr + \varepsilon_{is} \quad (11)$$

In the derivation described earlier, q_j is the real protein concentration in the adsorption phase based on the adsorption-phase volume. According to hypothesis (7), it is related to the experimentally determined adsorption amount (Q_j) based on the volume of a porous adsorbent volume as

$$q_j = \frac{Q_j}{\theta_j} \quad (12)$$

So, substitution of Eq. 12 into Eq. 11 yields

$$\mu_i^{s} = RT\ln(N_AV_i) + RT\ln\left(\frac{Q_i}{\theta_i}\right) - RT - RT\ln\left(\frac{\nu_{fi}}{\Lambda_i^3}\right) + \frac{1}{2}N_A\varepsilon_{sh} + N_A^2\sum_{j=1,\ldots,n}\left\{\eta_{ij}\frac{Q_j}{\theta_j}\int_V u_{ij}(r)4\pi r^2 dr\right\} + \varepsilon_{is} \quad (13)$$

This equation can be further simplified to

$$\mu_i^{s} = \mu_i^{s\Theta} + RT\ln\left(\frac{Q_i}{\theta_i}\right) + RT\sum_{j=1,\ldots,n}\eta_{ij}k_{ij}\frac{Q_j}{\theta_j} \quad (14)$$

where the standard chemical potential of adsorbed protein and the parameter k_{ij} descriptive of the interactions between adsorbed protein molecules is expressed by Eqs. 15 and 16, respectively.

$$\mu_i^{s\Theta} = RT\ln\left(\frac{N_AV_i\Lambda_i^3}{\nu_{fi}}\right) - RT + \frac{1}{2}N_A\varepsilon_{sh} + \varepsilon_{is} \quad (15)$$

$$k_{ij} = \frac{N_A}{k_BT}\left(\int_V u_{ij}(r)4\pi r^2 dr\right) \quad (16)$$

The chemical potential of protein i in an ideal bulk solution is

$$\mu_i^{b} = \mu_i^{b\Theta} + RT\ln c_{b,i} \quad (17)$$

When the adsorption is in equilibrium

$$\mu_i^{s} = \mu_i^{b} \quad (18)$$

Substituting Eqs. 14 and 17 into Eq. 18, we obtain the ST model formula as

$$c_{b,i} = \alpha_iQ_i\exp\left(\sum_{j=1,\ldots,n}\eta_{ij}k_{ij}\frac{Q_j}{\theta_j}\right) \quad (19)$$

where k_{ij} and α_i are expressed by Eqs. 16 and 20, respectively

$$\alpha_i = \frac{N_AV_i\Lambda_i^3}{2.72\nu_{fi}\theta_i}\exp\left(\frac{\frac{1}{2}N_A\varepsilon_{sh} - \mu_i^{b\Theta}}{RT} + \frac{\varepsilon_{is}}{RT}\right) \quad (20)$$

In the case of single protein (component 1) adsorption, η_{11} equals 1 and Eq. 19 is simplified to

$$c_{b,1} = \alpha_1 Q_1 \exp\left(\frac{k_{11} Q_1}{\theta_1}\right) \tag{21}$$

where

$$\alpha_1 = \frac{N_A V_1 \Lambda_1^3}{2.72 \nu_{f1} \theta_1} \exp\left(\frac{\frac{1}{2} N_A \varepsilon_{sh} - \mu_1^{b\Theta}}{RT}\right) \exp\left(\frac{\varepsilon_{1s}}{RT}\right) \tag{22}$$

$$k_{11} = \frac{N_A}{k_B T} \int_V u_{11}(r) 4\pi r^2 dr \tag{23}$$

The validity of the ST model formula (Eq. 21) is tested by experimental adsorption equilibrium data of a single protein, bovine serum albumin (BSA).

Experimental

Ion exchanger

DEAE Spherodex M (BioSepra, Cergy-Saint-Christophe, France) was used to evaluate the ST model. DEAE Spherodex M is a composite ion exchanger of a rigid silica matrix with large pores. This matrix is coated with dextran polymer, with flexible dextran chains extending inside the pores of the silica matrix. The ion-exchange groups are attached to the dextran chains. When proteins are adsorbed, the pores in the silica matrix will be filled with an effective mixture of proteins and dextran chains. In other words, the adsorption occurs in the volume of the pores. This is a convincing supportive argument for hypotheses (2) and (7), that is, that all molecules in the adsorption phase are well mixed and present in the pore volume.

Parameters related to the ion-exchanger

The adsorbent properties related to the model evaluation were determined experimentally. The wet adsorbent density was measured to be 1.26 g.mL^{-1} with a pycnometer at 25°C. The specific area of the dry adsorbent was determined to be 15.4 m^2.g^{-1} by mercury intrusion porosimetry (Quantachrome Poremaster-60, Quantachrome Corporation, USA). The ratio of the dry weight to the wet weight of the adsorbent was estimated at 0.51 by measuring the mass of a constant amount of adsorbent before and after drying under vacuum. So, the specific surface area of the wet adsorbent was 0.51 × 15.4 m^2.g^{-1} = 7.85 m^2.g^{-1}. The ion-exchange capacity was determined at 53.0 mmol.L^{-1} by the titration curve method.[14] Determined by the batch-diffusion method,[15] the effective porosity of adsorbent for BSA was estimated at 0.616.[14]

Adsorption equilibrium experiments

Adsorption of BSA (Sigma, St. Louis, MO, USA) on DEAE Spherodex M was performed using the stirred batch adsorption method at 25°C. The experimental procedure has been described previously.[14] The liquid phases used for making up protein solutions were 10 mmol/L Tris-HCl buffer (pH 7.40), 10 mmol/L phosphate buffers (pH 7.36 and 6.79), and 10 mmol/L acetate buffers (pH 6.00, 5.84 and 5.26). The ionic strength of the buffers was adjusted by adding NaCl up to 130 mmol/L. Prior to an adsorption experiment, the ion exchanger was equilibrated by the corresponding buffer overnight, and the buffer pH was measured after adsorption equilibrium. By the careful experimental design, the pH value in a single isotherm measurement was kept constant. Thus, BSA adsorption isotherms at different pH values and ionic strengths were obtained for the evaluation of the theoretical model. The ionic strengths of 10 mmol/L phosphate buffers were 16 mmol/L at pH 7.36 and 13 mmol/L at pH 6.79; the ionic strengths of 10 mmol/L Tris-HCl and the acetate buffers were all 10 mmol/L.

Results

Determination of model parameters

As described in the experimental chapter, adsorption isotherms of BSA to DEAE Spherodex M were measured in three different buffers of six different pH values. At each pH value, the experiments were carried out at three to six ionic strengths between 10–140 mmol/L. Thus, 25 adsorption isotherms predicting the relationship between Q_1 and $c_{b,1}$ with 177 data points obtained (Figure 1). With each of the adsorption isotherms, the model parameters α_1 and k_{11} in Eq. 21 can be obtained by fitting the ST model to the experimental data with the Solver tool embedded in the MS Excel 2000, resulting in 25 groups of the α_1 and k_{11} values. Here, it should be noted that k_{11} is sensitive to the isotherms in cases of high-protein adsorption amount when protein-protein interaction in the adsorption phase is strong. However, in less favorable adsorption conditions (for example, acetate buffer of pH 6.00, I = 140mmol/L and acetate buffer of pH 5.26, I = 110 mmol/L), because protein adsorption amount is low, the model fitting is not sensitive to k_{11}. Considering that the electrostatic interactions between adsorbed protein molecules will not be evident at the low pH and high-ionic strengths, it is reasonable to assume k_{11}, to be zero in those less favorable cases. With the values of α_1 and k_{11}, the adsorption amount of BSA can be calculated from Eq. 21. Figure 1 shows a comparison between the model predictions and experimental data for each isotherm. As can be seen, good agreement between the predicted and the measured BSA adsorption isotherms is presented at each pH and ionic strength. The standard deviation (SD) of the predicted Q_1 values from those of the measured Q_1 is estimated at 0.111, smaller than the SD value (0.215) predicted from the SMA model.[16]

Influence of liquid-phase conditions on α_1

In an infinitely dilute protein solution ($c_{b,1} \to 0$), the adsorbed protein would also approach infinitesimal ($Q_1 \to 0$). Thus, we can derive the following equation from Eq. 21.

$$\frac{1}{\alpha_1} = \lim_{c_{b,1} \to 0} \frac{Q_1}{c_{b,1}} \tag{24}$$

Equation 24 indicates that $1/\alpha_1$ is physically the equilibrium coefficient of protein at infinitely dilute solution, and represents

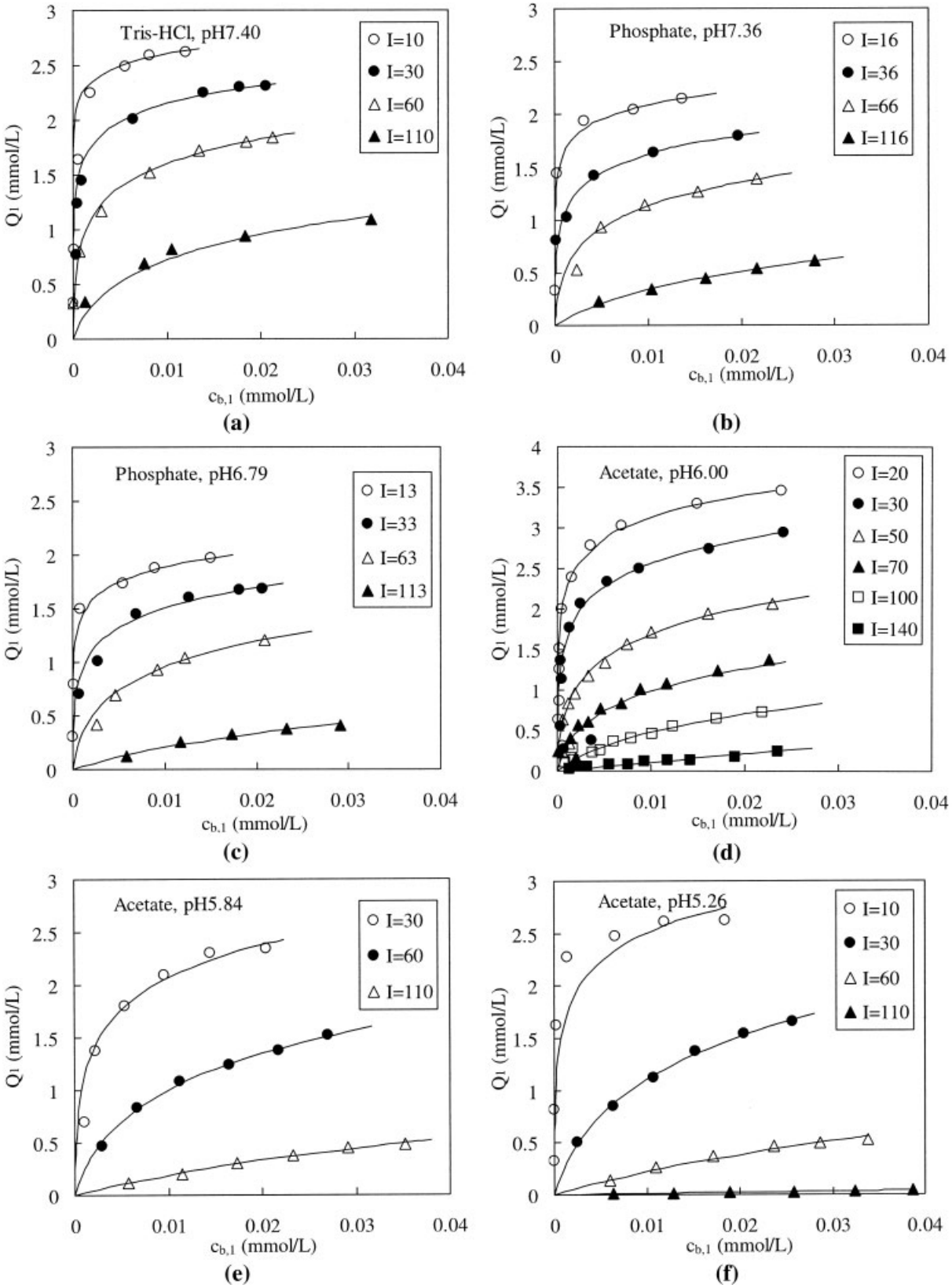

Figure 1. Adsorption isotherms of BSA to DEAE Spherodex M at different pH values and ionic strengths: (a) Tris-HCl buffer, pH 7.40, (b) phosphate buffer, pH 7.36, (c) phosphate buffer, pH6.79, (d) acetate buffer, pH6.00, (e) acetate buffer, pH5.84, and (f) acetate buffer, pH5.26.

The solid lines are calculated by fitting the ST model (Eq. 21) to the experimental data.

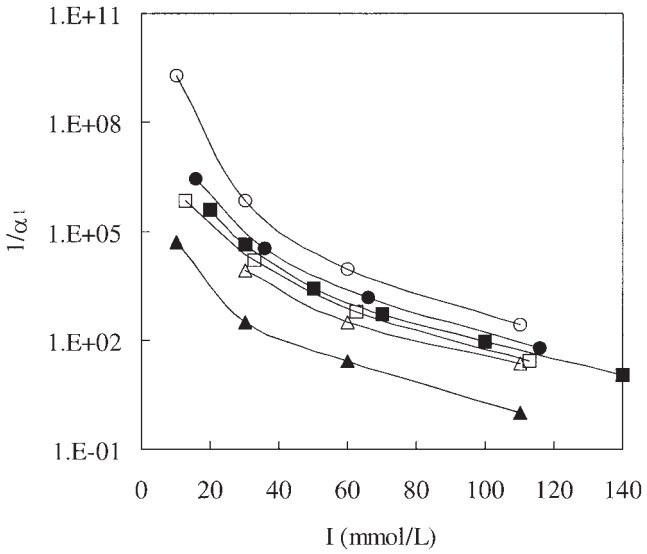

Figure 2. Dependence of $1/\alpha_1$ on the liquid-phase ionic strength in different buffers.

(○) Tris-HCl buffer, pH 7.40; (●) phosphate buffer, pH 7.36; (□) phosphate buffer, pH6.79; (■) acetate buffer, pH6.00; (△) acetate buffer, pH5.84; (▲) acetate buffer, pH5.26.

the adsorption affinity of the protein. Smaller α_1 means larger $1/\alpha_1$, and, hence, higher adsorption affinity. Liquid-phase conditions, such as pH and ionic strength could influence electrostatic interactions between protein and adsorption interface, resulting in the changes of ε_{1s}, and, thus, alter the $1/\alpha_1$ value as Eq. 22 indicates. Figure 2 shows $1/\alpha_1$ as a function of ionic strength in different buffers. It is readily understood that $1/\alpha_1$ decreases with ionic strength because protein adsorption affinity decreases with increasing ionic strength due to the electrostatic screening effect that reduces protein-adsorbent electrostatic attraction at high-ionic strength.[17,18] For the effect of pH, we can observe two general changing tendencies of $1/\alpha_1$.

First, $1/\alpha_1$, or in other words, the adsorption affinity, generally decreases with decreasing pH in the same buffer (phosphate or acetate). This is easily understood because the liquid-phase pH changes protein charge z_p, remarkably. BSA is an acidic protein with an isoelectric point (pI) of 4.7.[19] At the experimental pH range (5.26–7.40), BSA is negatively charged, and the net charge decreases with decreasing pH. So, the electrostatic attraction between BSA, and adsorbent surface is weaker at lower pH. Second, although the liquid-phase pH values are approximately the same, $1/\alpha_1$ is distinctly larger in Tris-HCl buffer (pH 7.40), than in phosphate buffer (pH 7.36), indicating higher adsorption affinity of BSA in Tris-HCl buffer than in phosphate buffer. This can be explained by the stronger effect of phosphate ions on the positively charged solid surface (DEAE groups). It has been stated that multivalent phosphate ions could combine with and screen the electropositive functional residuals of anion exchange adsorbent effectively, lowering the zeta potential of the adsorption interface, thus, weakening the electrostatic attraction between protein and anion exchange adsorbent markedly.[20] Due to the same reason, the value of $1/\alpha_1$ is even somewhat smaller in phosphate buffer of pH 6.79 than in the acetate buffer of pH 6.00.

Influence of liquid-phase conditions on k_{11}

k_{11} is descriptive of the interactions between adsorbed protein molecules. It is commonly accepted that proteins interact with each other in solution of high-concentrations, and similarly, there exist protein-protein interactions in an adsorption phase.[21-23] Ratnayake and Regnier[21] found that modification of an adsorbent surface by a protein could change the retention of proteins in chromatography, which is indicative of the presence of interactions between adsorbed proteins. As to adsorbed protein molecules of the same charge sign, electrostatic repulsions commonly occur, which is proven by calorimetric experiments.[23] Liquid-phase conditions can influence the electrostatic interaction between adsorbed protein molecules, namely u_{11}, and, thus, they can affect k_{11} value as indicated in Eq. 23.

Figure 3 shows the effect of pH and ionic strength on the value of k_{11}. It can be seen that the changing trend of k_{11} is similar to that of $1/\alpha_1$. That is, k_{11} decreases with decreasing liquid-phase pH and increasing ionic strength. With the decrease of pH, BSA become less negatively charged, so electrostatic repulsion between adsorbed BSA molecules is weakened. With the increase of ionic strength, the screening effect by coions is also strengthened, leading to the weakening of the electrostatic repulsion between adsorbed BSA molecules. There have been some reports verifying this trend on the interaction between adsorbed protein molecules.[22-24] For example, experiments of BSA adsorption to anion exchange adsorbent PEI-1000-1 showed that the adsorption process was more exothermic in the case of KCl addition than in the case of salt free. This phenomenon indicates the remarkable screening effect of small ions on adsorbed proteins.[23] In addition, the fact that smaller second virial coefficients of proteins were obtained by chromatography experiments at higher ionic strength[24] tes-

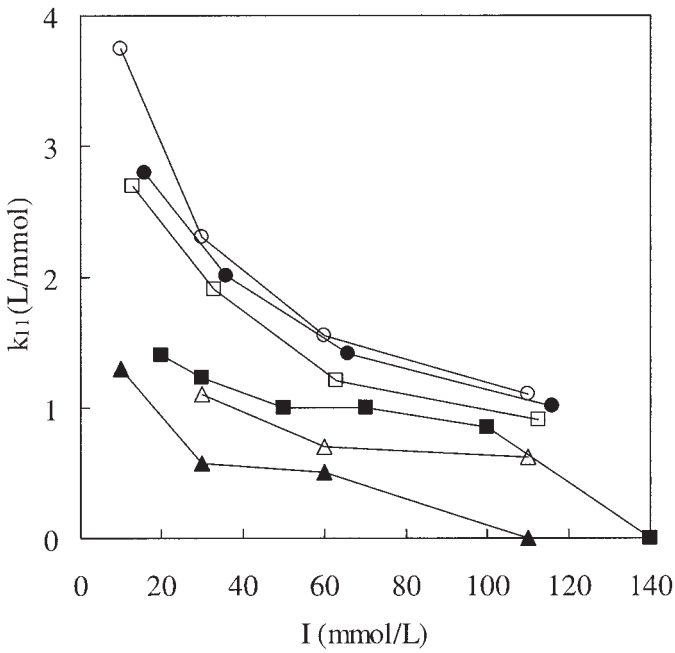

Figure 3. Dependence of k_{11} on the liquid-phase ionic strength in different buffers.

Symbols are the same as in Figure 2.

tifies the weakening electrostatic interaction between adsorbed protein molecules with increasing ionic strength.

Discussion

The earlier results have qualitatively indicated the reasonability of the model parameters as a function of pH and ionic strength. It is, thus, worthwhile quantitatively discussing more about their thermodynamic meanings because they are physically defined as Eqs. 22 and 23. The following is our primary attempts to this end.

In the definition of (Eq. 22), most thermodynamic factors are constant for the isothermic adsorption system. For instance, Λ_1 and ε_{sh} are constant because they are only dependent on temperature, ν_{f1} is independent of ionic strength as indicated by the assumption in the model derivation that ν_{fj} does not change with the molecule number. If we further assume that $\mu_1^{b\Theta}$ is constant, the only parameter dependent on ionic strength will be protein-adsorbent interaction potential ε_{1s}. So, the following relation is derived from Eq. 22

$$d\ln(1/\alpha_1) = -\frac{1}{RT}d\varepsilon_{1s} \tag{25}$$

By now, the models describing protein-adsorbent interactions in ion-exchange chromatography could be mainly classified into two categories: One was based on the stoichiometric law describing the interactions as simple columbic potential between the so-called protein characteristic charge and charged adsorption sites of adsorbent,[2-5] and the other was based on nonstoichiometric law treating the interactions as the electrical double layers potential between protein molecules and uniformly charged adsorption interface.[6,25-28] The "slab" model proposed by Ståhlberg et al.[6] that considered protein-adsorbent electrostatic interaction is frequently cited in literature due to its simplicity. According to this model, the minimum value of free energy ΔG_m in the process moving the two parallel "slabs" from infinity to be in contact is expressed as

$$\frac{\Delta G_m}{A_p} = -\frac{\sigma_p^2}{\kappa\varepsilon_0\varepsilon_r}, \text{ when } -\sigma_p<\sigma_s \tag{26a}$$

$$\frac{\Delta G_m}{A_p} = -\frac{\sigma_s^2}{\kappa\varepsilon_0\varepsilon_r}, \text{ when } -\sigma_p>\sigma_s \tag{26b}$$

where

$$A_p = 2\pi r_p^2 \tag{27}$$

$$\kappa = \left(\frac{\rho_w N_A e^2}{k_B T\varepsilon_0\varepsilon_r}\right)^{0.5} I^{0.5} \tag{28}$$

$$\sigma_p = \frac{z_p e}{4\pi r_p^2} \tag{29}$$

$$\sigma_s = 10^{-6}\times\frac{\Gamma N_A}{m_s\rho_s A_s}e \tag{30}$$

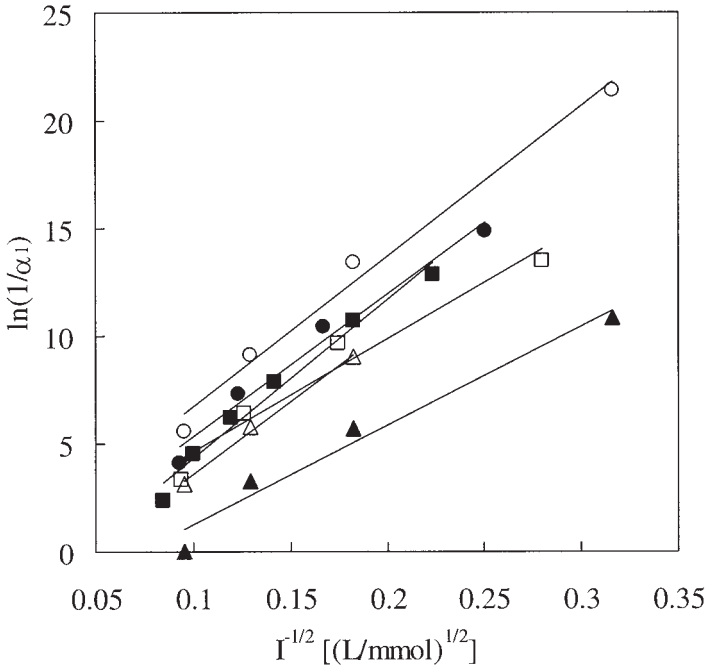

Figure 4. Relationship between $\ln(1/\alpha_1)$ and $I^{-0.5}$ in different buffers.

Symbols are the same as in Figure 2.

We estimate the parameters in these equations as follows. z_p is calculated with the formulas proposed by Scatchard et al.[29] and Tanford et al.,[30] and r_p is estimated at 2.69×10^{-9} m for BSA on the basis of its molecular volume.[31] In this experimental system, σ_s is estimated at 0.514 C/m^2, and the maximum $|\sigma_p|$ is calculated to be 2.78×10^{-2} C/m^2 by Eq. 29. So the relation of $-\sigma_p < \sigma_s$ holds, and Eq. 26a should be adopted. If only electrostatic interaction acts between protein and adsorbent, we have

$$\varepsilon_{1s} = N_A\Delta G_m \tag{31}$$

Substituting Eq. 26a and Eqs. 27 to 29 into Eq. 31 yields the following expression of

$$\varepsilon_{1s} = -(RT)^{0.5}\frac{e}{8\pi r_p^2}(\varepsilon_0\varepsilon_r\rho_w)^{-0.5}z_p^2 I^{-0.5} \tag{32}$$

Combining Eq. 32 and Eq. 25, we obtain the following relationship

$$\frac{d\ln(1/\alpha_1)}{d(I^{-0.5})} = \frac{e}{8\pi r_p^2}(\varepsilon_0\varepsilon_r\rho_w RT)^{-0.5}z_p^2 \tag{33}$$

Equation 33 indicates that $\ln(1/\alpha_1)$ should linearly increase with $1^{-0.5}$ if the righthand-side of the equation is constant. This is demonstrated by Figure 4, and the slopes and correlation coefficients of the straight lines are shown in Table 1. In all the cases, the correlation coefficients are larger than 0.95, indicating a good correlation of the straight lines described by Eq. 33 to the experimental data. In addition, the slopes of the straight

Table 1. Slopes of the Straight Lines in Figure 4 and the Correlation Coefficients of Eq. 33 to the Experimental Data

Buffer	Slopes in Figure 4 [(mmol/L)$^{1/2}$]	R^2
Tris-HCl, pH 7.40	69.8	0.987
Phosphate, pH 7.36	66.3	0.978
Phosphate, pH 6.79	53.1	0.953
Acetate, pH 6.00	73.2	0.980
Acetate, pH 5.84	67.0	0.996
Acetate, pH 5.26	46.1	0.966

lines are the values of the righthand-side of Eq. 33. In the same buffer (phosphate or acetate), the slope decreases with decreasing pH due to the reduced net charge z_p. In different buffers whose pH values are apart from the protein's isoelectric point, the slopes are in the order of acetate buffer (pH6.00), Tris-HCl buffer and phosphate buffer. The reason is not clear, and it needs further investigation.

Next, we discuss more about the other model parameter (k_{11}). As can be seen from Eq. 23, k_{11} is only related to the electrostatic interaction potential $u_{11}(r)$. $u_{11}(r)$ is expressed in Yukawa form as [32]

$$u_{11}(r) = k_B T \frac{B_{pp}}{r} r_p \exp[-\kappa(r - 2r_p)] \tag{34}$$

where the Yukawa coefficient B_{pp} is written as

$$B_{pp} = \left(\frac{4\pi k_B T \varepsilon_0 \varepsilon_r r_p}{e^2}\right)\left(4\gamma + \frac{2}{\kappa r_p}\gamma^3\right)^2 \tag{35}$$

In Eq. 35, γ is expressed as a function of the surface potential of protein molecules, ψ_p

$$\gamma = \tanh\left(\frac{\psi_p}{4}\right) \tag{36}$$

where ψ_p is determined by solving Eq. 37

$$\frac{\sigma_p}{\varepsilon_0 \varepsilon_r \kappa (k_B T/e)} = 2 \sinh\frac{\psi_p}{2} + \frac{4}{\kappa r_p}\tanh\left(\frac{\psi_p}{4}\right) \tag{37}$$

Substitution of Eq. 34 into Eq. 23 gives

$$k_{11} = 4\pi N_A r_p B_{pp} \int_V r \exp[-\kappa(r - 2r_p)]dr = 4\pi N_A r_p B_{pp}\left(\frac{2r_p}{\kappa} + \frac{1}{\kappa^2}\right) \tag{38}$$

Thus, if z_p is known at a given ionic strength and liquid-phase pH, we can calculate k_{11} from Eq. 38 combining Eqs. 28, 29, and 35 to 37. It should be noted that z_P in Eq. 38 (Eq. 29) is the effective protein charge in the adsorption phase, which may be different from that in the bulk solution. The value of z_p in bulk solution (that is, $z_{p,bulk}$,) can be determined by titration method, but the value of z_p in the adsorption phase (that is, $z_{p,ads}$) is hard to measure experimentally. We have tested using $z_{p,bulk}$ as a substitute of $z_{p,ads}$. for the calculation of k_{11}. Here, the values of $z_{p,bulk}$ are calculated according to Scatchard et al.[29] and Tanford et al.[30] In the calculation, the binding of chloride and acetate ions on BSA is considered, and the binding of acetate ions on BSA molecules is assumed to equal that of chloride ions.[33] The results are summarized in Table 2. It can be seen that $z_{p,bulk}$ increases with increasing ionic strength because the binding of chloride ions is considered. In phosphate buffer (pH 7.36) of ionic strength 36 mmol/L, the two values are in good agreement. In Tris-HCl and phosphate buffers of higher ionic strength ($\geq$60 mmol/L) and the three acetate buffers, the calculated is smaller than obtained by fitting the ST model to the experimental data. At low-ionic strength (about 10 mmol/L) in Tris-HCl and phosphate buffers, the situation becomes opposed to this. These can be explained by the following analysis.

First, Cl^- concentration in the adsorption phase (the diffuse electrical double layer of the positively charged adsorbent surface) is higher than that in the bulk liquid phase. Thus, more Cl^- binds to BSA molecule in the adsorption phase, resulting in higher net charge of BSA, and stronger electrostatic repulsion between the adsorbed BSA molecules than those calculated, based on the bulk liquid-phase condition (that is, $k_{11,a} > k_{11,b}$). Second, unlike the statement in model hypothesis (4), the short-range interaction between protein molecules is really affected by the distance between protein molecules, so it is influenced by protein adsorption concentration. Accordingly, although k_{11} is defined in the model derivation as electrostatic interaction between the adsorbed protein molecules, the fitted values of $k_{11,a}$ should also include the contribution of short-range interaction between adsorbed protein molecules. At high-protein adsorption concentration (low-ionic strength/high-pH value), protein-protein distance is short, leading to evident short-range attraction between protein molecules in the adsorption phase. This lessens the fitted k_{11} to some extent. The ealrier two factors are in contradiction to each other. When the impact of the first factor is dominant, there will be $k_{11,a} > k_{11,b}$. This corresponds to the cases in Tris-HCl and phosphate buffers of higher-ionic strength ($\geq$60 mmol/L), and the three acetate buffers. When the second factor is dominant, there will be $k_{11,a} < k_{11,b}$. This corresponds to the cases of low-ionic strength in Tris-HCl and phosphate buffers.

Conclusions

A statistical thermodynamic model (ST model) has been developed for the nonlinear multicomponent protein adsorption equilibrium on ion-exchanger. The model takes account of protein-adsorbent interactions and lateral protein-protein interactions in the adsorption phase, and agrees with the nonstoichiometric nature of the electrostatic adsorption of protein. All the model parameters have clear physical meanings, so the model captures the adsorption mechanism. The effect of buffer type, pH and ionic strength on the model parameters that describe protein adsorption affinity and the interactions between adsorbed protein molecules are reasonably interpreted by the electrostatic and thermodynamic theories. For practical application, however, the model parameters must be estimated by fitting to the experimental data. Therefore, it is still a challenge to find an efficient way to predict the model parameters, and the model needs further improvement by incorporat-

Table 2. Comparison of the Values of k_{11} Estimated from the ST Model and Calculated from Eq. 38

Buffer	I (mmol/L)	$z_{p,bulk}$	$k_{11,a}$ (L/mmol)	$k_{11,b}$ (L/mmol)	RD^c (%)
Tris-HCl, pH 7.40	10	−16.1	3.75	9.66	158
	30	−17.1	2.30	2.69	17.0
	60	−18.5	1.55	1.31	−15.5
	110	−20.1	1.10	0.707	−35.7
Phosphate, pH 7.36	16	−15.4	2.80	4.89	74.6
	36	−16.5	2.01	2.02	0.533
	66	−17.9	1.41	1.09	−22.5
	116	−19.6	1.01	0.631	−37.6
Phosphate, pH 6.79	13	−9.98	2.69	2.82	4.81
	33	−11.7	1.90	1.20	−36.8
	63	−13.5	1.20	0.695	−42.1
	113	−15.3	0.900	0.416	−53.8
Acetate, pH 6.00	20	−6.52	1.40	0.708	−49.4
	30	−7.33	1.23	0.543	−55.9
	50	−8.53	0.996	0.386	−61.2
	70	−9.40	0.992	0.304	−69.4
	100	−10.4	0.850	0.233	−72.6
	140	−11.3	0	0.176	—
Acetate, pH 5.84	30	−6.59	1.10	0.440	−60.0
	60	−8.25	0.699	0.287	−58.9
	110	−9.87	0.614	0.186	−69.7
Acetate, pH 5.26	10	−1.37	1.30	0.0715	−94.5
	30	−3.12	0.571	0.100	−82.5
	60	−4.63	0.500	0.0919	−81.6
	110	−6.14	0	0.0733	—

$k_{11,a}$ is estimated by fitting the ST model to the experimental data as in Figure 1.
$k_{11,b}$ is calculated from Eq. 38 combining Eqs. 28, 29 and 35 to 37 with $z_{p,bulk}$ listed in the table.
RD stands for relative deviation defined by $RD = (k_{11,b} - k_{11,a})/k_{11,a} \times 100\%$.

ing other molecular interactions, such as hydrophobic and van der Waals interactions. Despite these limitations, the model formulism is expected to find applications in the modeling of electrostatic adsorption chromatography of proteins, especially for multicomponent nonlinear systems. Hence, further work should direct toward model evaluation for application to multicomponent adsorption equilibria.

Acknowledgment

This work was supported by the Natural Science Foundation of China (No. 20476082), and the Doctoral Program Foundation for Universities, as well as the Program for Changjiang Scholars and Innovative Research Team in the University from the Ministry of Education of China.

Notation

A = Helmholtz free energy, J
A_p = effective interaction area of a protein molecule with adsorption surface, m^2
A_s = specific area of dry adsorbent, m^2/g
c = protein concentration, mmol/L
e = electron charge, C
ΔG_m = minimum value of free energy in the process moving two parallel charged slabs from infinity to be in contact, J
I = ionic strength, mmol/L
k_B = Boltzmann constant, 1.38×10^{-23} J/K
m_s = parameter defined in Eq. 16, descriptive of interactions between adsorbed proteins i and j
m_s = ratio of dry weight to wet weight of adsorbent
N_A = Avogadro's number
N_i = molecule number of the i-th species
qi = mole concentration in adsorption phase, mmol/L
Qi = experimental adsorption amount, mmol/L
r = distance between a pair of protein molecules i and j
r_p = radius of protein molecule, m
R = ideal gas constant, 8.314 J/mol·K
T = absolute temperature, K
$u_{ij}(r)$ = electrostatic interaction potential of a pair of protein molecules i and j with distance r
v_{fi} = effective volume of molecules of j-th species, m^3
V = volume, m^3
V_j = adsorption phase volume of protein j, m^3
$\bar{W}$ = mean configurational potential energy of the system, with each molecule at the center of its cell
$\bar{W}_{ele}$ = contribution of long-range electrostatic interaction to $\bar{W}$
$\bar{W}_{ele,pp}$ = contribution of protein-protein electrostatic interaction to $\bar{W}_{ele}$
$\bar{W}_{ele}^{\inf}$ = contribution of electrostatic interaction to $\bar{W}$ when protein molecules are infinitely apart
$\bar{W}_{sh}$ = contribution of short-range interaction to $\bar{W}$
z_p = net charge of protein
Z = canonical partition function

Greek letters

α_i = parameter defined in Eq. 20, inverse of equilibrium coefficient of protein at infinite dilution
Γ = ion-exchange capacity, mmol/L
ε_0 = dielectric permittivity of vacuum, 8.854×10^{-12} F/m
$\varepsilon(0)$ = potential energy of interaction of a molecule at its cell center with other molecules, J per molecule
$(1/2)\varepsilon_{ele,i}$ = mean electrostatic interaction potential of each molecule of protein i, J per protein molecule
ε_{is} = interactions between protein i and adsorption interface, J/mol
ε_r = relative dielectric permittivity of solvent (78.4 for water at 25°C)
$(1/2)\varepsilon_{sh}$ = mean short-range interaction potential of each molecule, J per molecule
θj = effective porosity of adsorbent to protein j
η_{ij} = correction factor for contribution of long-range electrostatic interaction potential between protein i and j due to the difference between their adsorption space
k = inverse Debye length, 1/m
Λ_j = characteristic parameter of the inherent energy of j-th species, m
μ_i^b = chemical potential of protein i in bulk solution, J/mol

μ_i^s = chemical potential of protein i in adsorption phase, J/mol
$\mu_i^{s'}$ = contribution of interactions between protein i and other molecules in adsorption phase to chemical potential of i, J/mol
$\rho_j(r)$ = number density of protein j at distance r from the central protein molecule
ρ_w = density of wet adsorbent, g/mL
ρ_s = number density of water molecules
σ = surface charge density of protein, C/m^2
σ = charge density of adsorption interface, C/m^2
ψ_p = surface potential of protein molecules, J

Literature Cited

1. Lan Q, Bassi AS, Zhu JX, Margaritis A. A modified Langmuir model for the prediction of the effects of ionic strength on the equilibrium characteristics of protein adsorption onto ion exchange/affinity adsorbents. *Chem Eng J.* 2001;81:179-186.
2. Kopaciewicz W, Rounds MA, Fausnaugh J, Regnier FE. Retention model for high-performance ion-exchange chromatography. *J Chromatogr.* 1983;266:3-21.
3. Li Y, Pinto NG. Influence of lateral interactions on preparative protein chromatography I. Isotherm behavior. *J Chromatogr A.* 1994;658:445-457.
4. Brooks CA, Cramer SM. Steric mass-action ion-exchange: displacement profiles and induced salt gradients. *AIChE J.* 1992;38:1969-1978.
5. Raje P, Pinto NG. Combination of the Steric Mass Action and Non-Ideal Surface Solution models for overload protein ion-exchange chromatography. *J Chromatogr A.*1997;760:89-103.
6. Ståhlberg J, Jönsson B, Horvath C. Theory for electrostatic interaction chromatography of proteins. *Anal Chem.* 1991;63:1867-1874.
7. Haggerty L, Lenhoff AM. Relation of protein electrostatics computations to ion-exchange and electrophoretic behavior. *J Phys Chem.* 1991;95:1472.
8. Norde W, Lyklema J. The adsorption of human plasma albumin and bovine pancreas ribonuclease at negatively charged polystyrene surfaces IV. The charge distribution in the adsorbed state. *J Colloid Interface Sci.* 1978;66:285-294.
9. Norde W, Lyklema J. Thermodynamics of protein adsorption theory with special reference to the adsorption of human plasma albumin and bovine pancreas ribonuclease at polystyrene surfaces. *J Colloid Interface Sci.* 1979;71:350-366.
10. Roth CM, Lenhoff A M. Electrostatic and van der waals contributions to protein adsorption: computation of equilibrium constants. *Langmuir.* 1993;9:962-972.
11. Bosma JC, Wesselingh JA. Available area isotherm. *AIChE J.* 2004; 50:848-853.
12. Hill TL. *An introduction to statistical thermodynamics*. Reading, Mass: Addison-Wesley Pub. Co.; 1960.
13. Hirtzel CS, Rajagopalan Raj. *Colloidal phenomena: Advanced topics*. Park Ridge, N. J., USA: Noyes Publications; 1985.
14. Chen WD, Dong XY, Sun Y. Analysis of diffusion models for protein adsorption to porous anion-exchange adsorbent. *J Chromatogr A.* 2002;962:29-40.
15. Zhang SP, Sun Y. Ionic strength dependence of protein adsorption to dye-ligand adsorbents. *AIChE J.* 2002;48:178-186.
16. Chen WD, Sun Y. Analysis of steric mass-action model for protein ion-exchange equilibrium. *J Chem Ind Eng* (China). 2002;53:88-91.
17. Huang JX, Schudel J, Guiochon G. Adsorption behavior of albumin and conalbumin on TSK-DEAE 5PW anion exchanger. *J Chromatogr A.* 1990;504:335-349.
18. Hashim MA, Chu KH, Tsan PS. Effects of ionic strength and pH on the adsorption equilibria of lysozyme on ion exchangers. *J Chem Tech Biotechnol.* 1995;62:253-260.
19. Reyes L, Bert J, Fornazero J, Cohen R, Heinrich L. Influence of conformational changes on diffusion properties of bovine serum albumin: A holographic interferometry study. *Colloids and Surfaces B: Biointerfaces.* 2002;25:99-108.
20. Luo Q, Andrade JD, Caldwell KD. Thin-layer ion-exchange chromatography of proteins. *J Chromatogr A.* 1998;816:97-105.
21. Ratnayake CK, Regnier FE. Lateral interaction between electrostatically adsorbed and covalently immobilized proteins on the surface of cation-exchange sorbents. *J Chromatogr A.* 1996;743:25-32.
22. Ortega-Vinuesa JL, Tengvall P, Lundström I. Molecular packing of HSA, IgG, and fibrinogen adsorbed on silicon by AFM imaging. *Thin Solid Films.* 1998;324:257-273.
23. Thrash ME Jr, Pinto NG. Characterization of enthalpic events in overloaded ion-exchange chromatography. *J Chromatogr A.* 2002; 944:61-68.
24. Teske CA, Blanch HW, Prausnitz JM. Chromatographic measurement of interactions between unlike proteins. *Fluid Phase Equilibria.* 2004; 219:139-148.
25. Ståhlberg J, Jönsson B, Horvath C. Combined effect of coulombic and van der waals interactions in the chromatography of proteins. *Anal Chem.* 1992;64:3118-3124.
26. Ståhlberg J, Appelgren U, Jönsson B. Electrostatic interactions between a charged sphere and a charged planar surface in an electrolyte solution. *J Colloid Interface Sci.* 1995;176:397-407.
27. Jönsson B, Ståhlberg J. The electrostatic interaction between a charged sphere and an oppositely charged planar surface and its application to protein adsorption. *Colloids Surf.* 1999;14:67-75.
28. Hallgren E, Kalman F, Farnan D, Horvath C, Ståhlberg J. Protein retention in ion-exchange chromatography: Effect of net charge and charge distribution. *J Chromatogr A.* 2000;877:13-24.
29. Scatchard G., Scheinberg IH, Armstrong SH Jr. Physical chemistry of protein solutions. IV. The combination of human serum albumin with chloride ion. *J Amer Chem Soc.* 1950;72:535-540.
30. Tanford C, Swanson SA, Shore WS. Hydrogen ion equilibria of bovine serum albumin. *J Amer Chem Soc.* 1955;77:6414-6421.
31. Bosma JC, Wesselingh JA. pH dependence of ion-exchange equilibrium of proteins. *AIChE J.* 1998;44:2399-2408.
32. Oberholzer MR, Stankovich JM, Carnie SL, Chan DYC, Lenhoff AM. 2-D and 3-D interactions in random sequential adsorption of charged particles. *J Colloid Interf Sci.* 1997;194:138-153.
33. Bosma JC. More efficient process chromatography. University of Groningen, Dept of Chem & Chem Eng; 2001. PhD Thesis.

Manuscript received May 13, 2005, and revision received Apr. 17, 2006.